

# CPM Specifications Document

## AAA Dissection:

OSMSC 0143\_0000

---

May 1, 2013

Version 1

Open Source Medical Software Corporation

© 2013 Open Source Medical Software Corporation. All Rights Reserved.

## 1. Clinical Significance & Condition

Hemodynamic may play an important role in other anomalies in the aorta. An overview of some of major anomalies has been provided below.

Both the thoracic and abdominal aorta are prone to the development of aneurysms and hemodynamic and biomechanical forces are thought to play a role in the progression of the disease and risk of rupture.

Rupture of Abdominal Aortic Aneurysms (AAA) carries a risk of death of up to 90%. They are more common in men and are present in 1.3% of men aged 45-54 and 12.5% of men 75-84 years old. They are present in 0% and 5.2% of women in respective age groups [1].

On the other hand, the prevalence of Thoracic aortic aneurysms is equal in men and women with an incidence rate of 10.4 per 100,000 person-years [1]. Thoracic aortic aneurysms can occur as a result of aortic dissection, which can occur anywhere in the aorta but more often occur in the thoracic aorta. Aortic dissection is a tear in the internal lining of the wall of the aorta. The prevalence of aortic dissection is estimated to be around 2.9-3.5% per 100,000 person-years, a majority of which are male [1].

Coarctation of the Aorta (CoA) refers to the narrowing of any section of the aorta; however, CoA is most commonly seen in the area immediately after the arch of the aorta, the site where the ductus arteriosus closes [2]. CoA is the fifth of most common cardiovascular defect at birth, though it may also develop as a result of other cardiovascular anomalies in infancy, adolescence, and early adulthood [3]. It accounts for 8-11% of congenital heart defects in the U.S and affects about 1 out of 10,000 individuals of all ages [4, 5]. Despite the various options for treatment, CoA has been associated with decreased in life expectancy and long term morbidity [4].

## 2. Clinical Data

Patient-specific volumetric image data was obtained to create physiological models and blood flow simulations. Details of the imaging data used can be seen in Table 1. See Appendix 1 for details on image data orientation.

Table 1 – Patient-specific volumetric image data details (mm)

OSMSC ID	Modality	Voxel Spacing			Voxel Dimensions			Physical Dimensions		
		R	A	S	R	A	S	R	A	S
0143_0000	CT	0.5859	0.5859	2.5000	512	512	256	300	300	640

Available patient-specific clinical data collected can be seen in Table 2.

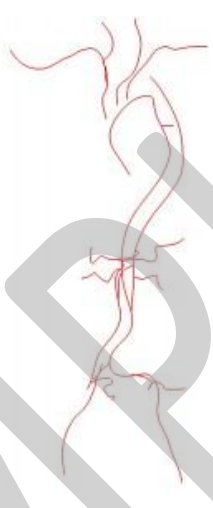
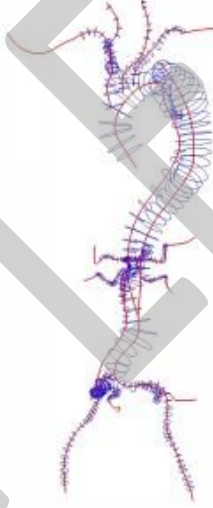
Table 2 – Available patient-specific clinical data

OSMSC ID	Age	Gender	Height (m)	Weight (kg)	HR (bpm)	Psys (mmHg)	Pdia (mmHg)
0143_0000	72	M	1.8	99.8	58	161	100

### 3. Anatomic Model Description

Anatomic models were created using customized SimVascular software (Simtk.org) and the image data described in Section 2. AAA models extend from the supraceliac aorta, include the splenic, hepatic, renal, superior and inferior mesenteric (when visible), and iliac arteries, and end before the femoral and profunda femoris artery bifurcation. See Appendix 2 for a description of modeling methods. See **Error! Reference source not found.** for a visual summary of the image data, paths, segmentations and solid model constructed.

Table 3 – Visual summary of image data, paths, segmentations and solid model.

OSMSC ID	Image Data	Paths	Paths and Segmentations	Model
ID: OSMSC0143 subID: 0000 Age: 72 Gender: M				

Details of anatomic models, such as number of outlets and model volume, can be seen in Table 4.

Table 4 – Anatomic Model details

OSMSC ID	Inlets	Outlets	Volume (cm <sup>3</sup> )	Surface Area (cm <sup>2</sup> )	Vessel Paths	2-D Segmentations
0143_0000	1	13	862.4662	1388.355	17	342

### 4. Physiological Model Description

In addition to the clinical data gathered for this model, several physiological assumptions were made in preparation for running the simulation. See Appendix 3 for details.

### 5. Simulation Parameters & Details

No simulation results available.

### 6. Simulation Results

No simulation results available.

## 7. References

- [1] Centers for Disease Control and Prevention, "Aortic Aneurysms Fact Sheet," 3 January 2011. [Online]. Available: [http://www.cdc.gov/dhbsp/data\\_statistics/fact\\_sheets/fs\\_aortic\\_aneurysm.htm](http://www.cdc.gov/dhbsp/data_statistics/fact_sheets/fs_aortic_aneurysm.htm). [Accessed 4 April 2012].
- [2] American Heart Association, "Coarctation of the Aorta," 24 January 2011. [Online]. Available: [http://www.heart.org/HEARTORG/Conditions/CongenitalHeartDefects/AboutCongenitalHeartDefects/Coarctation-of-the-Aorta-CoA\\_UCM\\_307022\\_Article.jsp#.TwX7UNR8AsK](http://www.heart.org/HEARTORG/Conditions/CongenitalHeartDefects/AboutCongenitalHeartDefects/Coarctation-of-the-Aorta-CoA_UCM_307022_Article.jsp#.TwX7UNR8AsK). [Accessed 5 January 2012].
- [3] American Heart Association, "Heart Disease and Stroke Statistics--2012 Update: A Report From the American Heart Association," *Circulation*, vol. 125, pp. e2-e220, 2012.
- [4] J. LaDisa, A. Figueroa, I. Vignon-Clementel, H. J. Kim, N. Xiao, L. Ellwein, F. Chan, J. Feinstein and C. Taylor, "Computational Simulations for Aortic Coarctation: Representative Results From a Sampling of Patients," *Journal of Biomedical Engineering*, vol. 133, 2011.
- [5] MDGuidelines, "Coarctation of the Aorta," [Online]. Available: <http://www.mdguidelines.com/coarctation-of-the-aorta>. [Accessed 06 January 2012].

# Appendix

## 1. Image Data Orientation

The RAS coordinate system was assumed for the image data orientation. Voxel Spacing, voxel dimensions, and physical dimensions are provided in the Right-Left (R), Anterior-Posterior (A), and Superior-Inferior (S) direction in all specification documents unless otherwise specified.

## 2. Model Construction

All anatomic models were constructed in RAS Space. The models are generated by selecting centerline paths along the vessels, creating 2D segmentations along each of these paths, and then lofting the segmentations together to create a solid model. A separate solid model was created for each vessel and Boolean addition was used to generate a single model representing the complete anatomic model. The vessel junctions were then blended to create a smoothed model.

## 3. Physiological Assumptions

Newtonian fluid behavior is assumed with standard physiological properties. Blood viscosity and density are given below in units used to input directly into the solver.

**Blood Viscosity:**  $0.04 \text{ g/cm} \cdot \text{s}^2$

**Blood Density:**  $1.06 \text{ g/cm}^3$

## 4. Simulation Parameters

Conservation of mass and Navier-Stokes equations were solved using 3D finite element methods assuming rigid and non-slip walls. All simulations were ran in cgs units and ran for several cardiac cycles to allow the flow rate and pressure fields to stabilize.

## 5. Outlet Boundary Conditions

### 5.1 Resistance Methods

Resistances values can be applied to the outlets to direct flow and pressure gradients. Total resistance for the model is calculated using relationships of the flow and pressure of the model. Total resistance is than distributed amongst the outlets using an inverse relationship of outlet area and the assumption that the outlets act in parallel.

### 5.2 Windkessel Model

In order to represent the effects of vessels distal to the CFD model, a three-element Windkessel model can be applied at each outlet. This model consists of proximal resistance ( $R_p$ ), capacitance ( $C$ ), and distal resistance ( $R_d$ ) representing the resistance of the proximal vessels, the capacitance of the proximal vessels, and the resistance of the distal vessels downstream of each outlet, respectively (Figure 1).

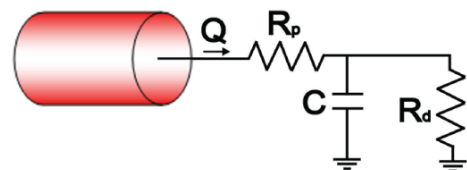


Figure 1 - Windkessel model

First, total arterial capacitance (TAC) was calculated using inflow and blood pressure. The TAC was then distributed among the outlets based on the blood flow distributions. Next, total resistance ( $R_t$ ) was calculated for each outlet using mean blood pressure and PC-MRI or calculated target flow ( $R_t = P_{\text{mean}} / Q_{\text{desired}}$ ). Given that  $R_t = R_p + R_d$ , total resistance was distributed between  $R_p$  and  $R_d$  adjusting the  $R_p$  to  $R_t$  ratio for each outlet.

SAMPLE